Toward a Low-Barrier Transition-Metal-Free Catalysis of Hydrogenation Reactions: A Theoretical Mechanistic Study of $HAlX_4$-Catalyzed Hydrogenations of Ethene (X = F, Cl, and Br)

Stefan Senger and Leo Radom*

Research School of Chemistry, Australian National University, Canberra, ACT 0200, Australia

Received: March 30, 2000

Ab initio molecular orbital theory at the MP2/6-311+G(3df,2p)//B3-LYP/6-31G(d) level has been used to study the transition-metal-free catalysis of the hydrogenation of ethene. Catalysis by HX, $(HX)_2$ and $HAlX_4$ (X = F, Cl, and Br) has been examined. Both concerted pathways and stepwise pathways involving CH_3-CH_2X-type intermediates have been characterized. The former are energetically preferred in the case of the HX- and $(HX)_2$-catalyzed reactions. However, for the $HAlX_4$-catalyzed hydrogenations, concerted and stepwise mechanisms are found to have similar barriers. The $HAlX_4$ species are found to be very effective hydrogenation catalysts, reducing the barrier for the hydrogenation of ethene from the value of 367 kJ mol^{-1} in the uncatalyzed process to less than 100 kJ mol^{-1} for all the halogens (X).

Introduction

Transition-metal-catalyzed homogeneous[1] and heterogeneous[2] hydrogenations are very intensively studied chemical reactions. One major reason for the interest taken in hydrogenation reactions is their great industrial importance.[3] As an example, in the Swiss-based chemical company Ciba Geigy (now Novartis), more than 90% of catalytic production processes in 1996 were hydrogenations.[4]

In total contrast to the transition-metal-catalyzed hydrogenations, there is very little known about transition-metal-free catalysis of hydrogenation reactions. In 1961, Walling and Bollyky[5] were the first to propose that strong acids catalyze the reaction of molecular hydrogen with unsaturated hydrocarbons. Three years later, they reported that isobutene and cyclohexene react with hydrogen in the presence of HBr and $AlBr_3$.[6] For the mechanism of these reactions, it was assumed that carbenium ions are the key intermediates.[6] In the postulated reaction sequence, the carbenium ions are formed through protonation of the double bond of the unsaturated substrate by the acid, and they subsequently react with a hydride ion from molecular hydrogen to form the hydrogenated product while a proton is regenerated.

In 1987, the first theoretical study of acid-catalyzed hydrogenations was undertaken by Bertrán and co-workers.[7] Choosing ethene as a prototype for an alkene and HF and H_3O^+ as acids of different strength, they studied the potential energy surface for hydrogenation reactions at the HF/3-21G level of theory. In both cases, the calculated reaction barriers are substantially reduced when compared with the uncatalyzed reaction of ethene with molecular hydrogen; with H_3O^+ the reaction is almost barrier-free. Although this result looks very promising, Bertrán and co-workers pointed out that a major challenge in finding suitable experimental conditions would be to avoid the addition of the acid to the double bond. Curiously enough, Walling and Bollyky[6] had already found a way to perform an HBr-catalyzed hydrogenation in the laboratory. As mentioned above, they used $AlBr_3$ as a co-catalyst.

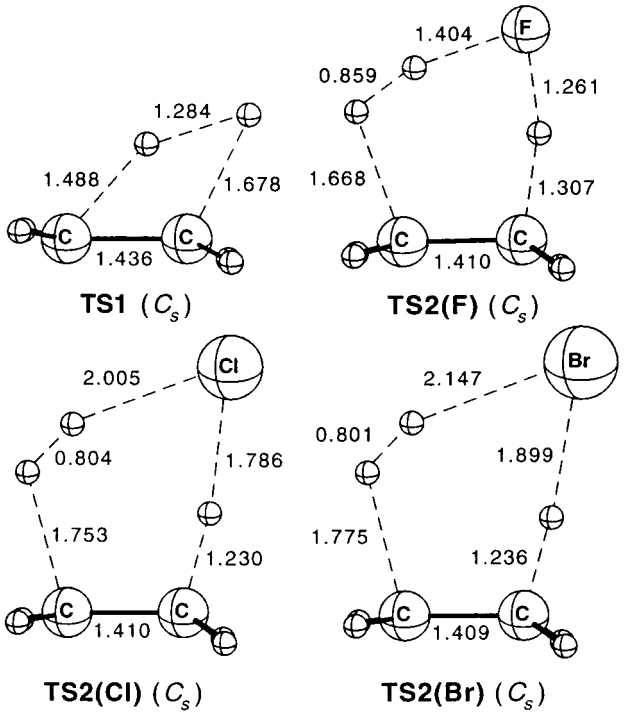

Figure 1. Selected B3-LYP/6-31G(d) bond lengths (Å) for the transition structures for the concerted uncatalyzed (**TS1**) and HX-catalyzed (**TS2(X)**; X = F, Cl, Br) hydrogenations of ethene.

How does the presence of an aluminum trihalide affect the reaction between molecular hydrogen, the hydrogen halide and the unsaturated substrate? The purpose of the present paper is to to attempt to answer this question and to gain a better understanding of this type of acid-catalyzed hydrogenation. This work represents part of our continuing interest in the catalysis of hydrogenation reactions, including model calculations for catalysis by enzymes[8] and zeolites.[9]

In the present theoretical investigation, we have chosen ethene as a prototypical alkene, studying its reaction with molecular

10.1021/jp001226r CCC: $19.00
Published on Web 07/18/2000

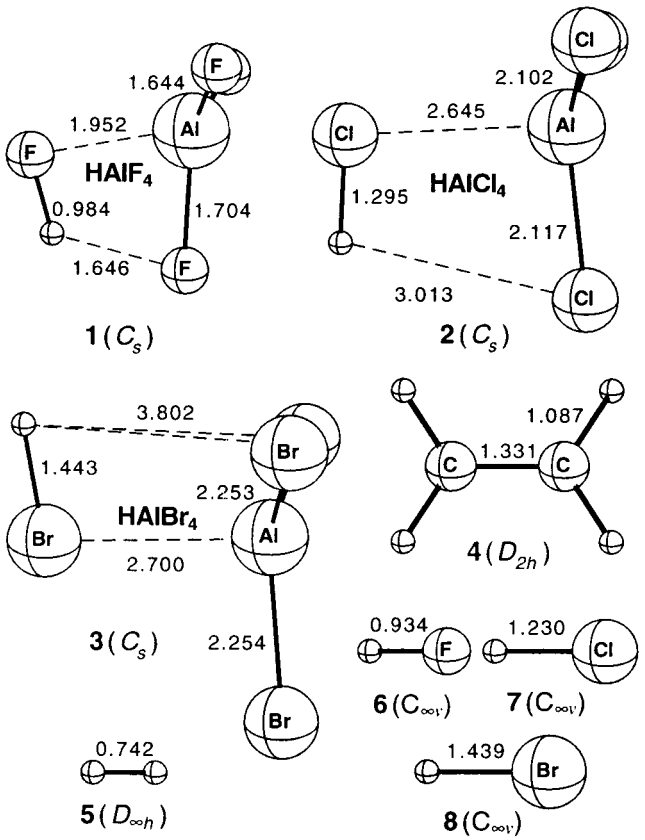

Figure 2. Selected B3-LYP/6-31G(d) bond lengths (Å) for $HAlX_4$, HX (X = F, Cl, Br), H_2. and ethene. Corresponding bond lengths for AlX_3 are 1.639 (X = F), 2.087 (X = Cl), and 2.231 (X = Br) Å.

TABLE 1: Calculated Overall Barriers at 0 K (kJ mol^{-1}) for the Uncatalyzed and Concerted HX-Catalyzed Hydrogenations of Ethene

	catalyst			
		HF	HCl	HBr
B3-LYP/6-31G(d)[a]	363	198	147	121
MP2/6-31G(d,p)[b]	390	264	212	171
B3-LYP/6-311+G(3df,2p)[a]	351	228	169	143
MP2/6-311+G(3df,2p)[a]	367	263	200	170
MP2/6-311+G(3df,2p)[b]	365	262	189	162
G2**	363	264	194	165

[a] Using B3-LYP/6-31G(d) optimized geometries. [b] Using MP2/6-31G(d,p) optimized geometries.

hydrogen in the presence of HX, $(HX)_2$, and HX-AlX_3, with X = F, Cl, and Br. Since the experiments reported for these reactions have been performed in solvents of low polarity, our gas-phase calculations may provide a meaningful comparative description.

Computational Details

Standard ab initio molecular orbital calculations[10,11] have been carried out with the GAUSSIAN 98 package of programs.[12] Geometry optimizations and frequency calculations were carried out with B3-LYP/6-31G(d), and were followed by single-point MP2/6-311+G(3df,2p) energy calculations. Unless otherwise noted, relative energies in this paper correspond to MP2/6-311+G(3df,2p) values at 0 K, calculated using the B3-LYP/6-31G(d) optimized geometries and incorporating scaled (by 0.9806)[13] B3-LYP/6-31G(d) zero-point vibrational energy (ZPVE) corrections. For the calculation of the thermal energy and entropy, scaling factors of 0.9989 and 1.0015, respectively, were used.[13] The intrinsic reaction coordinate (IRC) method was employed to confirm the two minima connected by each transition structure.

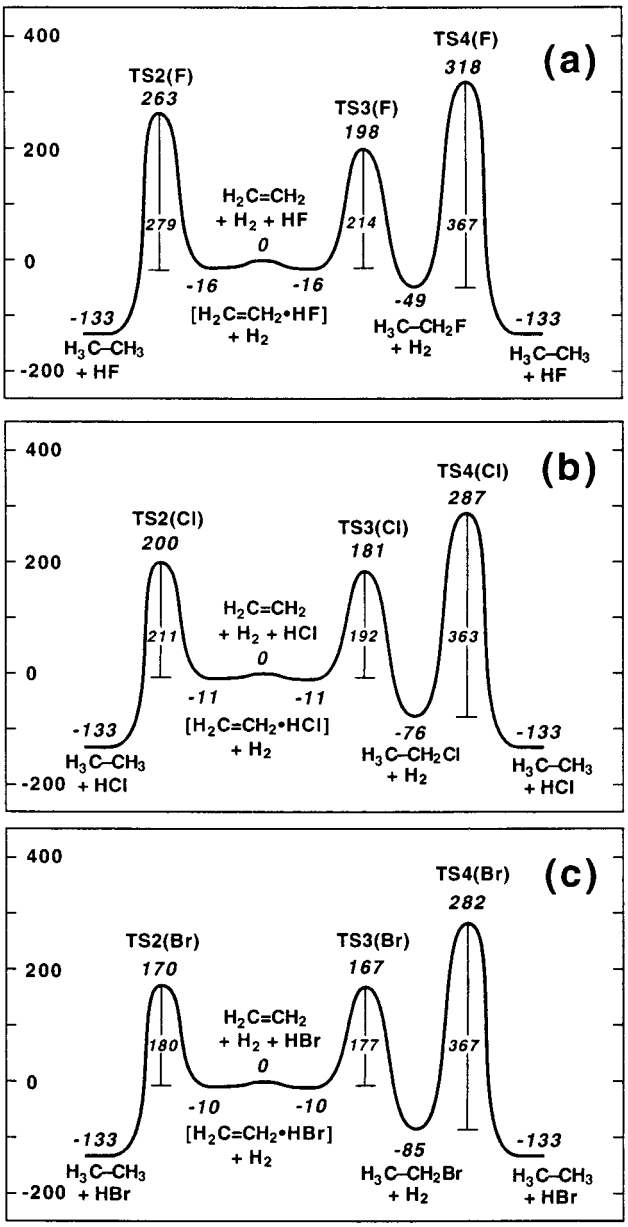

Figure 3. Schematic energy profiles for (a) the HF-catalyzed, (b) the HCl-catalyzed, and (c) the HBr-catalyzed hydrogenations of ethene. MP2/6-311+G(3df,2p)//B3-LYP/6-31G(d) relative energies at 0 K are given in kJ mol^{-1}.

GAUSSIAN 98 archive entries for B3-LYP/6-31G(d) optimized geometries of relevant equilibrium structures and transition structures, and calculated B3-LYP/6-31G(d) total energies and ZPVEs and MP2/6-311+G(3df,2p)//B3-LYP/6-31G(d) total energies are given in Tables S1 and S2 of the Supporting Information.

To provide benchmark energies for comparison, we have used a modified version of G2, which we will refer to as G2**, in a number of prototypical cases. G2** employs MP2(fc)/6-31G(d,p) geometries and frequencies (scaled by 0.9608)[13] rather than the standard G2 choices of MP2/6-31G(d) and HF/6-31G(d), respectively.

Results and Discussion

HX-Catalyzed Hydrogenation of Ethene. Using the HF/3-21G transition structure for the concerted HF-catalyzed hydro-

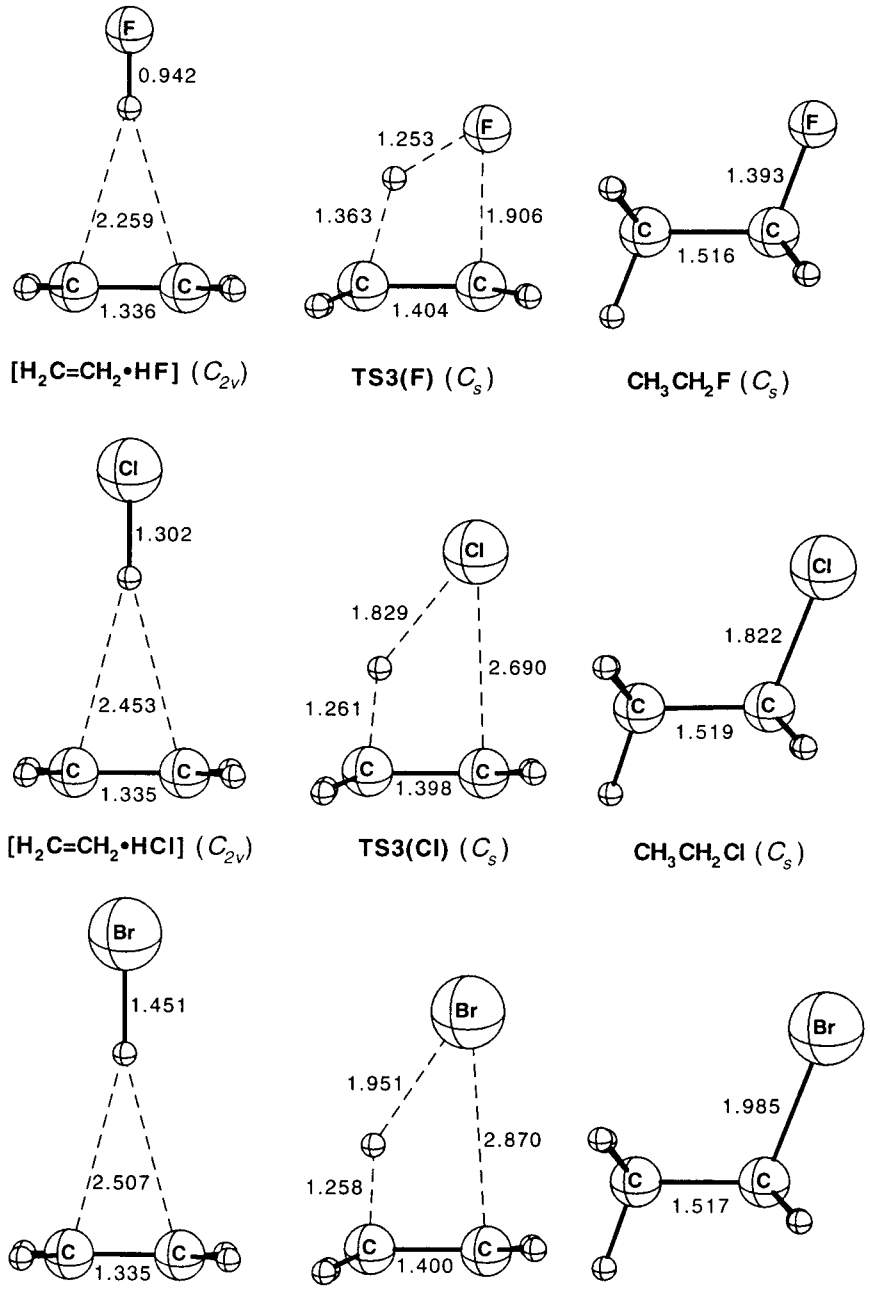

Figure 4. Selected B3-LYP/6-31G(d) bond lengths (Å) for the complexes [$H_2C{=}CH_2{\cdot}HX$], the transition structures **TS3(X)** for the addition of HX to ethene, and for the resulting ethyl halides (X = F, Cl, Br).

genation of ethene located by Bertrán and co-workers[7] as a starting geometry, we reoptimized it at the B3-LYP/6-31G(d) level of theory. In addition, we located the analogous transition structures for the concerted HCl- and HBr-catalyzed hydrogenations of ethene. The resultant structures **TS2(F)**, **TS2(Cl),** and **TS2(Br)**, together with the transition structure **TS1** for the uncatalyzed hydrogenation of ethene, are displayed in Figure 1. The structures of the reactants are given in Figure 2 for comparison purposes. As can be seen, the transition structures for the concerted HX-catalyzed hydrogenations of ethene have very similar geometries. For example, the C−C bond lengths of 1.410 Å in **TS2(F)**, 1.410 Å in **TS2(Cl)** and 1.409 Å in **TS2(Br)** are practically identical. Similarly, the H−X bond is extended by 35% in **TS2(F)**, 45% in **TS2(Cl),** and 32% in **TS2(Br)**, while the H−H bond is lengthened by 8% in **TS2(Cl)** and **TS2(Br)** and by 16% in **TS2(F)**. On the other hand, the H−H bond in the transition structure for the uncatalyzed hydrogenation of ethene (**TS1)** is lengthened to a substantially greater extent (by approximately 70%). This indicates that the transition structures for the concerted HX-catalyzed hydrogenations occur early on the reaction pathway, at least with respect to cleavage of the H−H bond.

To assess the likely quality of the B3-LYP and MP2 energies for the HX-catalyzed hydrogenation reactions, we calculated the barriers for the concerted HF-, HCl-, and HBr-catalyzed hydrogenations of ethene, as well as for the uncatalyzed reaction, with B3-LYP/6-31G(d), MP2/6-31G(d,p), B3-LYP/6-311+G(3df,2p)//B3-LYP/6-31G(d), MP2/6-311+G(3df,2p)//B3-LYP/6-31G(d), MP2/6-311+G(3df,2p)//MP2/6-31G(d,p), and G2**. The results are grouped together in Table 1. Although B3-LYP/6-31G(d) rather fortuitously yields the same barrier as G2** for the uncatalyzed hydrogenation of ethene, the barriers for the HX-catalyzed reactions are underestimated by approximately 40−60 kJ mol^{-1}. With B3-LYP/6-311+G(3df,2p)//B3-LYP/6-31G(d) the differences from G2** are reduced to about 12−26 kJ mol^{-1}, whereas for MP2/6-311+G(3df,2p)//B3-LYP/

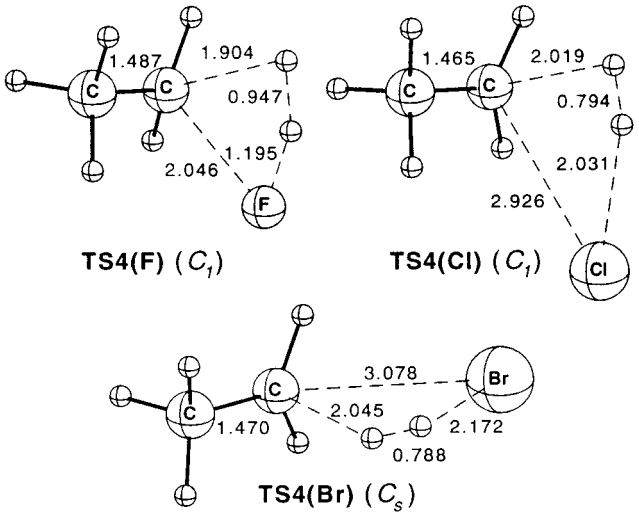

Figure 5. Selected B3-LYP/6-31G(d) bond lengths (Å) for the transition structures **TS4(X)** for the uncatalyzed hydrogenolyses of the ethyl halides CH_3CH_2X (X = F, Cl, Br).

6-31G(d) the maximum deviation from the G2** barriers is just 6 kJ mol^{-1}. We therefore chose to use the MP2/6-311+G(3df,-2p)//B3-LYP/6-31G(d) level of theory for energy considerations throughout the present study.

The comparisons in Table 1 show that the barriers for the HX-catalyzed hydrogenations decrease in going from HF to HCl to HBr. Compared with the calculated barrier for the uncatalyzed hydrogenation of ethene, the barrier for the concerted HX-catalyzed hydrogenations are reduced by 28% in the presence of HF, by 46% if HCl is the catalyst and by a slightly larger value of 54% for HBr. Schematic energy profiles for these hydrogenations are displayed in Figure 3.

An alternative reaction that ethene may undergo in the presence of HX is the addition of the HX "catalyst" to the double bond.[14,15] The B3-LYP/6-31G(d) geometries of the complexes [$H_2C{=}CH_2{\cdot}HX$], the transition structures (**TS3(X)**) for the additions of HX to ethene and of the resulting ethyl halides CH_3CH_2X (X = F, Cl, Br) are given in Figure 4. The barriers for the reaction of ethene with HF, HCl, and HBr are included in Figure 3 and can be seen to be smaller than the barriers for the corresponding HX-catalyzed hydrogenation reactions in all three cases, although the difference for HBr (Figure 3c) is just 3 kJ mol^{-1}. However, since the HX addition reactions are bimolecular, as opposed to the termolecular concerted HX-catalyzed hydrogenations, the addition of HX to the double bond will be even more favored at higher temperatures for entropical reasons. For example, at 298 K (p = 1 atm) the calculated free energy of activation (relative to the separate reactants) for the addition of HBr to ethene is approximately 50 kJ mol^{-1} smaller than the corresponding value for the concerted HBr-catalyzed hydrogenation reaction. For these reasons, it seems likely that even in the presence of molecular hydrogen most of the ethene, instead of being catalytically hydrogenated, should initially react with the HX "catalyst" to form an ethyl halide.

Starting from the ethyl halides, the hydrogenolysis of the C−X bonds provides an alternative means for achieving the hydrogenation of ethene. The transition structures for these reactions are shown in Figure 5. Whereas it was straightforward to locate **TS4(F)** and **TS4(Cl)** on the B3-LYP/6-31G(d) potential energy surface, our initial optimizations aimed at locating **TS4(Br)** led to the transition structure for the concerted HBr-catalyzed hydrogenation of ethene **TS2(Br)** (cf. Figure 1). After constraining the geometry to C_s symmetry, we located the structure **TS4(Br)** shown in Figure 5 which has two imaginary frequencies, one being 47.7i cm^{-1} with A″ symmetry and the other having the very small value of 0.00051i. A subsequent MP2/6-31G(d) optimization and frequency calculation showed that a structure analogous to **TS4(Br)** (with C_s symmetry) is a true transition structure on the MP2/6-31G(d) potential energy surface. Therefore, we used the B3-LYP/6-31G(d) geometry for **TS4(Br)** shown in Figure 5 to perform the MP2/6-311+G(3df,-2p) single-point energy calculation.

A comparison between the B3-LYP/6-31G(d) and MP2/6-31G(d) structures for **TS4(X)** shows that the two methods yield similar transition structures for **TS4(F)**, but lead to somewhat different structures for **TS4(Cl)** and **TS4(Br)** The MP2/6-31G(d) transition structures for the uncatalyzed hydrogenolyses of ethyl chloride and ethyl bromide have C_s symmetry with a dihedral angle (between the two carbon atoms, the halogen atom and the hydrogen atom adjacent to the halogen) of 180°, whereas this dihedral angle is −95.4° in the transition structure **TS4(Cl)** optimized with B3-LYP/6-31G(d) (see Figure 5).

As in the case of **TS4(Br)**, we used the B3-LYP/6-31G(d) structure depicted in Figure 5 to calculate the MP2/6-311+G-(3df,2p) single-point energies for both **TS4(F)** and **TS4(Cl)**.[16] The results are included in Figure 3. For all three ethyl halides under investigation, the barriers for the hydrogenolysis of the C−X bond are (coincidentally) nearly identical to the barrier (367 kJ mol^{-1}) for the uncatalyzed hydrogenation of ethene (cf. Table 1). The relative energies (compared with ethene, hydrogen plus the hydrogen halide) of the transition structures for the hydrogenolyses of the ethyl halides **TS4(X)** are much higher (by 55−112 kJ mol^{-1}) than the relative energies for the transition structures for the concerted hydrogenations of ethene **TS2(X)**. Therefore, even though ethene may react initially with HX to form an ethyl halide, the lowest energy pathways to form ethane are those via the transition structures **TS2(X)** for the concerted HX-catalyzed hydrogenations and not via the transition structures **TS4(X)** for the hydrogenolyses of the ethyl halides.

$(HX)_2$-Catalyzed Hydrogenation of Ethene. From the theoretical studies of Bertrán and co-workers[14] and Sordo and co-workers,[15] it is known that the presence of a second HX molecule lowers the barrier for the addition of HX to ethene. This encouraged us to study the influence of HX on the reaction of molecular hydrogen with the corresponding ethyl halide. To do so, we calculated the energy profiles for the reactions between ethene, molecular hydrogen, and the hydrogen halide dimers $(HX)_2$ (X = F, Cl, Br). This included a reoptimization with B3-LYP/6-31G(d) of the stationary points described in the literature[14,15] for the reactions of ethene with $(HX)_2$ to give the complexes [$CH_3CH_2X{\cdot}HX$]. The B3-LYP/6-31G(d) geometries for the hydrogen halide dimers $(HX)_2$, the complexes [$H_2C{=}CH_2{\cdot}2HX$], the transition structures for the HX-catalyzed additions of HX to ethene **TS5(X),** and for the resulting complexes [$CH_3CH_2X{\cdot}HX$] are given in Figure 6. The transition structures **TS6(X)** and **TS7(X)** for the concerted reactions of ethene with H_2 plus $(HX)_2$ are displayed in Figure 7. The energy profiles for the $(HX)_2$-catalyzed hydrogenations of ethene are grouped together in Figure 8 and the transition structures **TS8(X)** for the HX-catalyzed hydrogenolyses of the ethyl halides are shown in Figure 9.

Whereas the second HX molecule plays an active role in the addition of $(HX)_2$ to the double bond of ethene and in the hydrogenolyses of the ethyl halides, as reflected in the substantial reductions in the barriers for these reactions (cf. Figure 8), the second HX molecule is less strongly involved in the preferred concerted $(HX)_2$-catalyzed hydrogenations of ethene

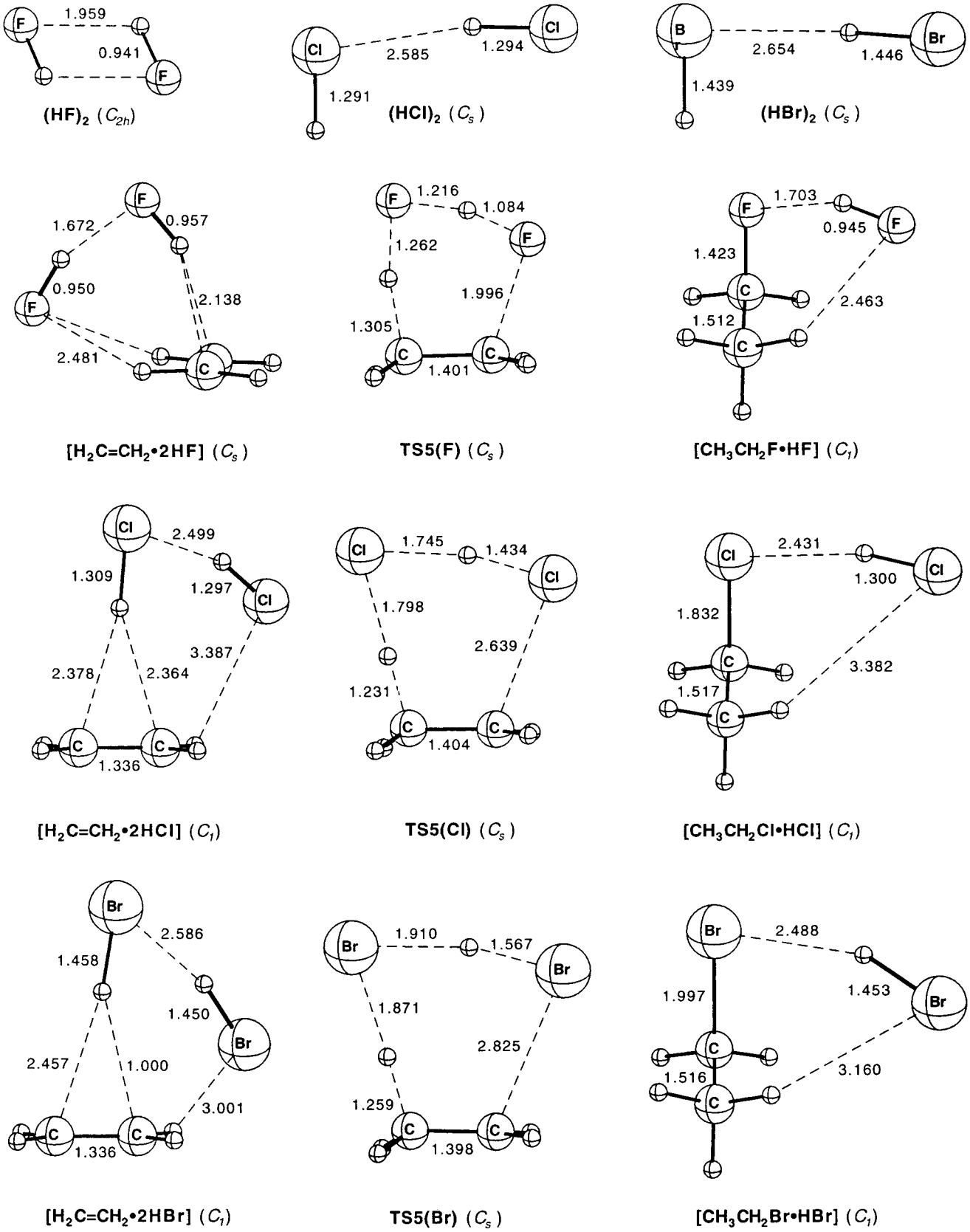

Figure 6. Selected B3-LYP/6-31G(d) bond lengths (Å) for the hydrogen halide dimers $(HX)_2$, the complexes $[H_2C{=}CH_2{\cdot}2HX]$, the transition structures **TS5(X)** for the HX-catalyzed addition of HX to ethene and the resulting complexes $[CH_3CH_2X{\cdot}HX]$ (X = F, Cl, Br).

via **TS6(X)** (see Figure 7) and the effects on the barriers are smaller (namely, barrier reductions of approximately 10%). The transition structures for these concerted $(HX)_2$-catalyzed hydrogenations **TS6(X)** closely resemble the transition structures **TS2(X)** for the HX-catalyzed hydrogenations, complexed with an additional HX. Alternative eight-membered cyclic transition structures **TS7(X)** for the concerted $(HX)_2$-catalyzed hydrogenations of ethene have also been characterized (also included in Figure 7). These are found to have energies (228, 223, and 199 kJ mol^{-1} for X = F, Cl, and Br, respectively), which are

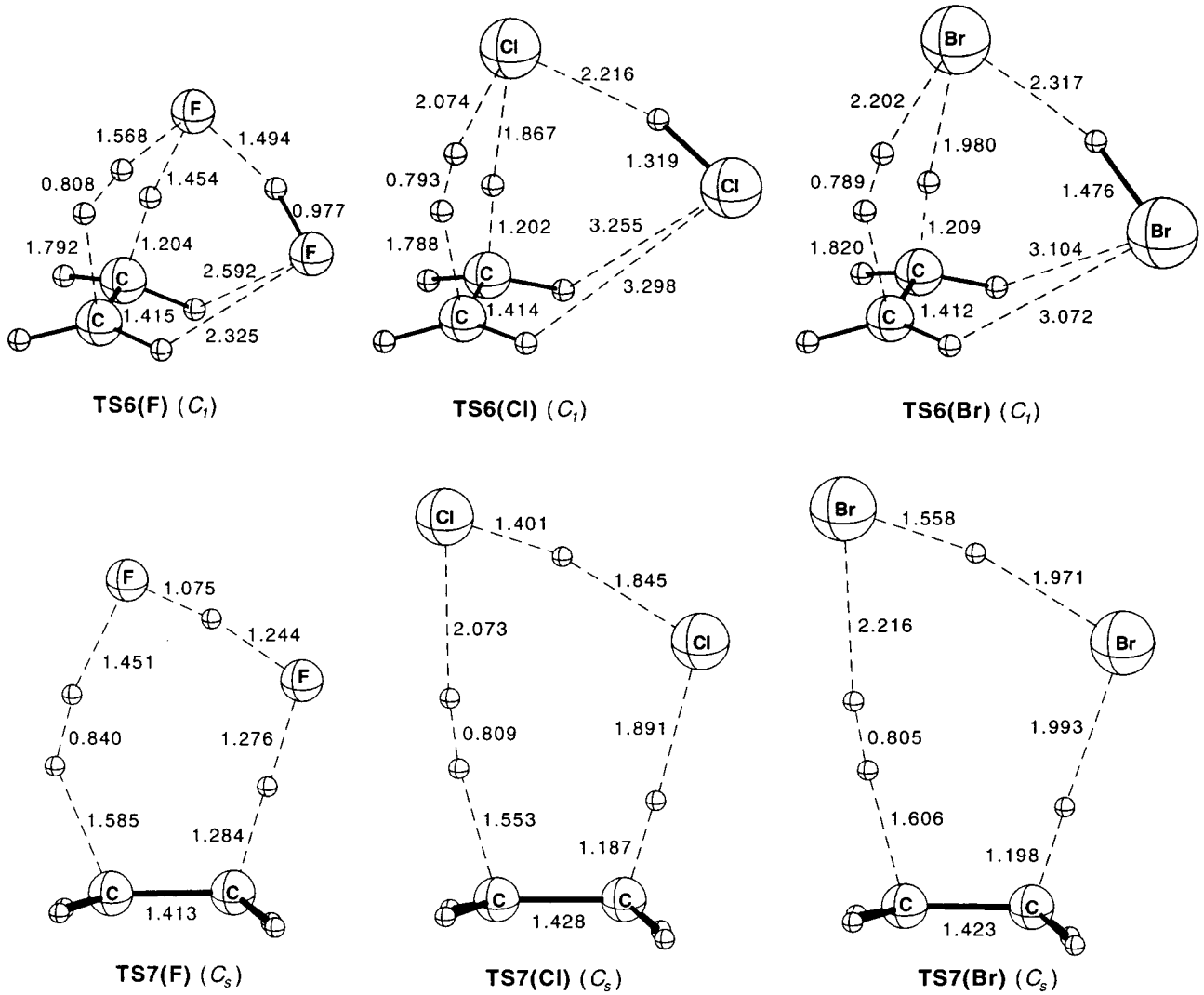

Figure 7. Selected B3-LYP/6-31G(d) bond lengths (Å) for the transition structures **TS6(X)** and **TS7(X)** for the concerted $(HX)_2$-catalyzed hydrogenation of ethene (X = F, Cl, Br).

comparable to or somewhat higher than corresponding values for **TS6(X)** (229, 182, and 157 kJ mol^{-1} for X = F, Cl, and Br, respectively; see Figure 8).

Even for the reaction catalyzed by $(HBr)_2$, where the effect of the second HX molecule in the stepwise reaction is largest, resulting in a reduction in the overall barrier for the stepwise hydrogenation from 282 to 185 kJ mol^{-1}, the concerted mechanism (with a barrier of 157 kJ mol^{-1}) is still energetically favored. Our calculations indicate that this should also be the case at room temperature. The calculated (overall) standard free energy of activation (T = 298.15 K, p = 1 atm) for the concerted $(HBr)_2$-catalyzed hydrogenation of ethene is 257 kJ mol^{-1}, compared with 288 kJ mol^{-1} for the two-step reaction via the complex [CH_3CH_2Br·HBr].

$HAlX_4$-Catalyzed Hydrogenation of Ethene. The calculated structures for the complexes [HX·AlX_3] (with X = F, Cl, and Br), to which we will refer as $HAlX_4$, are included in Figure 2. All three $HAlX_4$ complexes have C_s symmetry, but they differ in that F−H and Cl−H are located cis relative to one of the Al−F or Al−Cl bonds in $HAlF_4$ and $HAlCl_4$, respectively (which is in accordance with previous theoretical studies, see refs 17 and 18), whereas Br−H is positioned trans to an Al−Br bond in $HAlBr_4$. To check whether the different structure of $HAlBr_4$ is an artifact of the B3-LYP/6-31G(d) method, we reoptimized all three complexes with MP2/6-31G(d,p) and were reassured to find that the MP2/6-31G(d,p) structural features are the same as those described above for the B3-LYP/6-31G(d) structures. The binding energies calculated at various theoretical levels for the $HAlF_4$, $HAlCl_4$ and $HAlBr_4$ complexes are compared with G2** results in Table 2. As can be seen, the MP2/6-311+G(3df,2p)//B3-LYP/6-31G(d) method used in this study yields results which are in good agreement with the G2** values.

The calculated structures for the complexes between $HAlX_4$ and ethene are shown in Figure 10. [$H_2C{=}CH_2$·$HAlF_4$] has C_s symmetry with the F−H bond of the hydrogen fluoride in a cis orientation with respect to an Al−F bond in the aluminum trifluoride moiety, in a manner similar to that in $HAlF_4$ (see Figure 2). [$H_2C{=}CH_2$·$HAlCl_4$] also has C_s symmetry but the orientation of the Cl−H bond relative to the Al−Cl bond has changed to trans. The [$H_2C{=}CH_2$·$HAlBr_4$] complex resembles [$H_2C{=}CH_2$·$HAlCl_4$] but has no symmetry. The binding energies for the complexes can be found in Figure 11.

The transition structures for the AlX_3-catalyzed additions of HX to ethene **TS9(X)** are also included in Figure 10. In contrast to the situation in the uncatalyzed addition of HX to a double bond (Figure 4), in **TS9(X)** only the hydrogen atom of the hydrogen halide HX binds to a carbon atom of the alkene. The halogen atom of the hydrogen halide is donated to the catalyst AlX_3, and one of the halogen atoms of the AlX_3 forms a bond

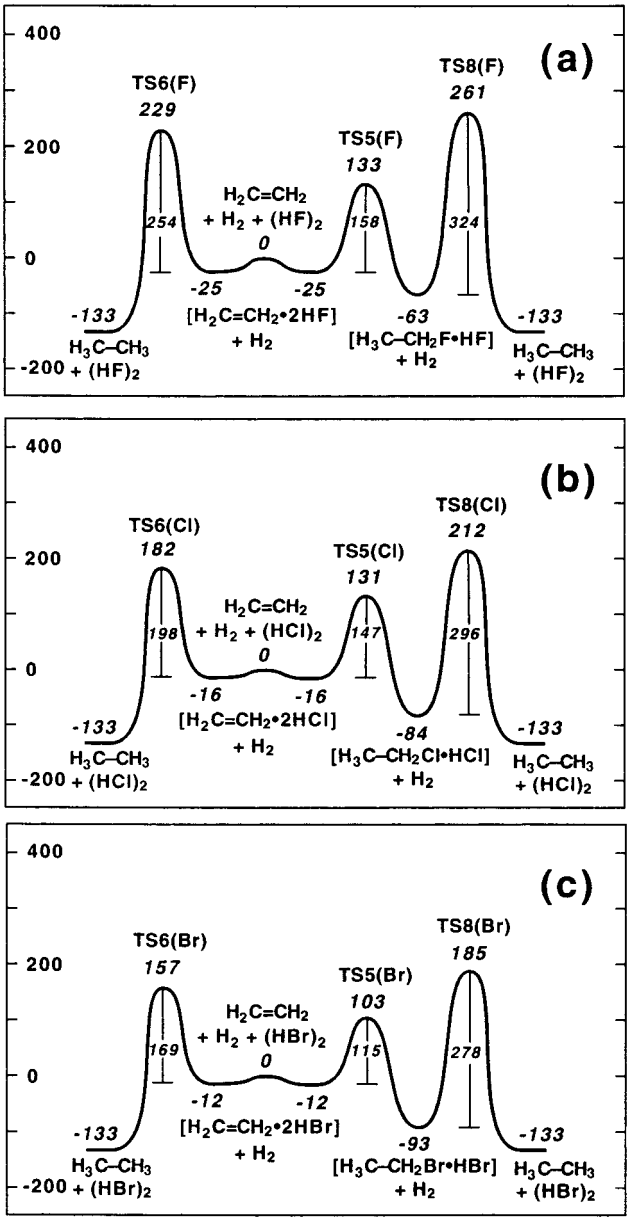

Figure 8. Schematic energy profiles for (a) the $(HF)_2$-catalyzed, (b) the $(HCl)_2$-catalyzed, and (c) the $(HBr)_2$-catalyzed hydrogenations of ethene. MP2/6-311+G(3df,2p)//B3-LYP/6-31G(d) relative energies at 0 K are given in kJ mol^{-1}.

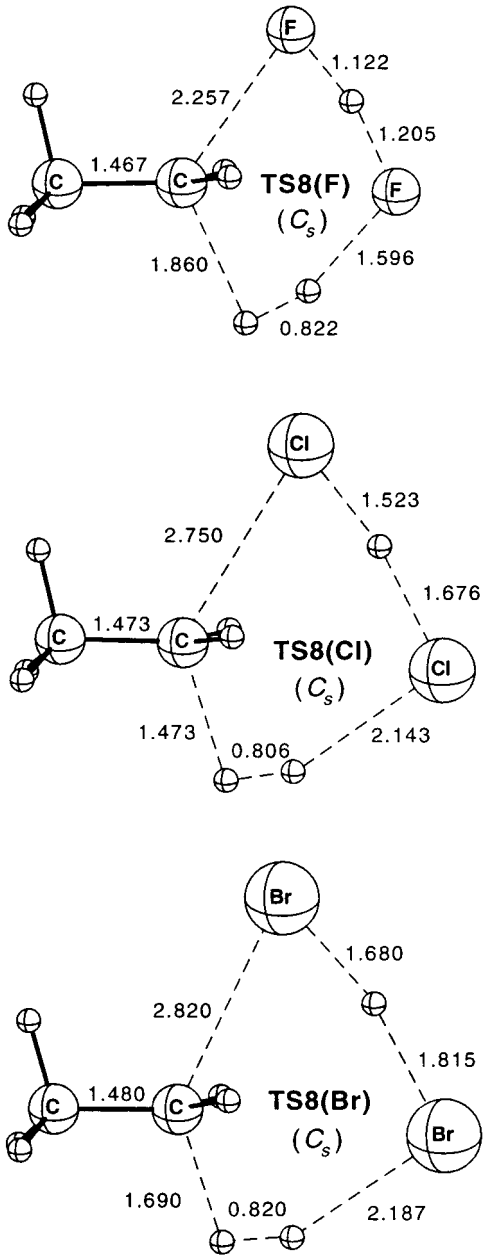

Figure 9. Selected B3-LYP/6-31G(d) bond lengths (Å) for the transition structures **TS8(X)** for the HX-catalyzed hydrogenolyses of the ethyl halides CH_3CH_2X (X = F, Cl, Br).

with the alkene. In this sense, the situation is very similar to the reaction of the HX dimer with ethene, where the hydrogen atom is provided by one HX molecule while the halogen atom originates from the second HX molecule of the dimer $(HX)_2$ (for details, see **TS5(X)** in Figure 6 and refs 14 and 15). There is thus a strong mechanistic similarity between the HX-catalyzed and the AlX_3-catalyzed additions of HX, but the effect is much larger in the latter (see Figure 11). For example, whereas the calculated (overall) barrier for the uncatalyzed addition of HBr to ethene is 167 kJ mol^{-1} (Figure 3c) and the corresponding barrier for the HBr-catalyzed reaction is still as much as 103 kJ mol^{-1} (Figure 8c), there is no (overall) barrier at all if the reaction is catalyzed by $AlBr_3$ (Figure 11c). We also note that whereas in **TS5(X)**, the forming C···H bond is shorter for X = Cl and Br than for X = F, the opposite behavior is observed for **TS9(X)**.

The products of the AlX_3-catalyzed addition of HX to ethene are the complexes of the resulting ethyl halides with the corresponding aluminum trihalide $[CH_3CH_2X{\cdot}AlX_3]$ (also included in Figure 10). The calculated lengths for the C−X bonds in the CH_3CH_2X moiety of the complexes $[CH_3CH_2X{\cdot}AlX_3]$ are about 7% longer for X = F and approximately 2% longer for X = Cl and Br compared with corresponding values for uncomplexed CH_3CH_2X (included in Figure 4). The calculated

TABLE 2: Calculated Binding Energies at 0 K (kJ mol^{-1}) for the Complexes $HAlF_4$, $HAlCl_4$ and $HAlBr_4$

	$HAlF_4$ $[HF{\cdot}AlF_3]$	$HAlCl_4$ $[HCl{\cdot}AlCl_3]$	$HAlBr_4$ $[HBr{\cdot}AlBr_3]$
B3-LYP/6-31G(d)[a]	106	21	57
MP2/6-31G(d,p)[b]	100	25	65
B3-LYP/6-311+G(3df,2p)[a]	51	17	8
MP2/6-311+G(3df,2p)[a]	55	35	31
MP2/6-311+G(3df,2p)[b]	60	36	30
G2**	61	34	26

[a] Using B3-LYP/6-31G(d) optimized geometries. [b] Using MP2/6-31G(d,p) optimized geometries.

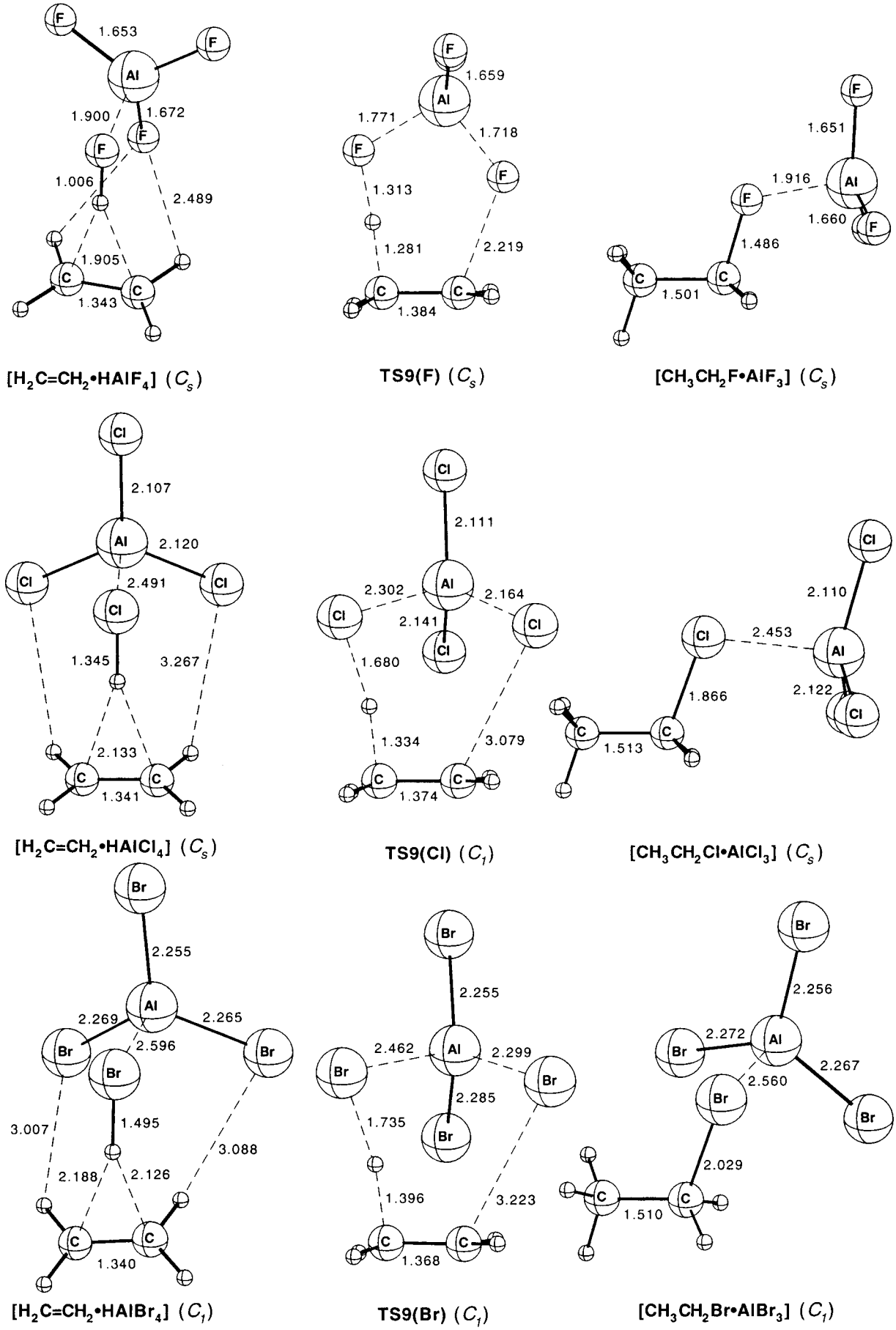

Figure 10. Selected B3-LYP/6-31G(d) bond lengths (Å) for the complexes [$H_2C{=}CH_2{\cdot}HAlX_4$], the transition structures **TS9(X)** for the AlX_3-catalyzed additions of HX to ethene, and the product complexes [$CH_3CH_2X{\cdot}AlX_3$] (X = F, Cl, Br).

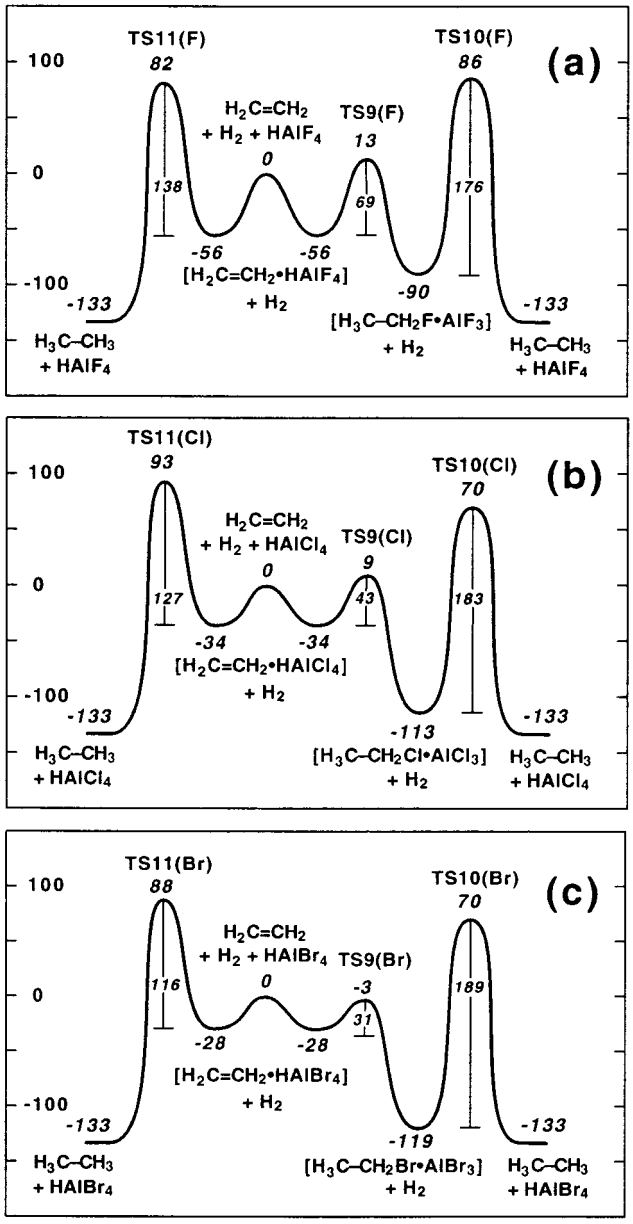

Figure 11. Schematic energy profiles for (a) the $HAlF_4$-catalyzed, (b) the $HAlCl_4$-catalyzed, and (c) the $HAlBr_4$-catalyzed hydrogenation of ethene. MP2/6-311+G(3df,2p)//B3-LYP/6-31G(d) relative energies at 0 K are given in kJ mol^{-1}.

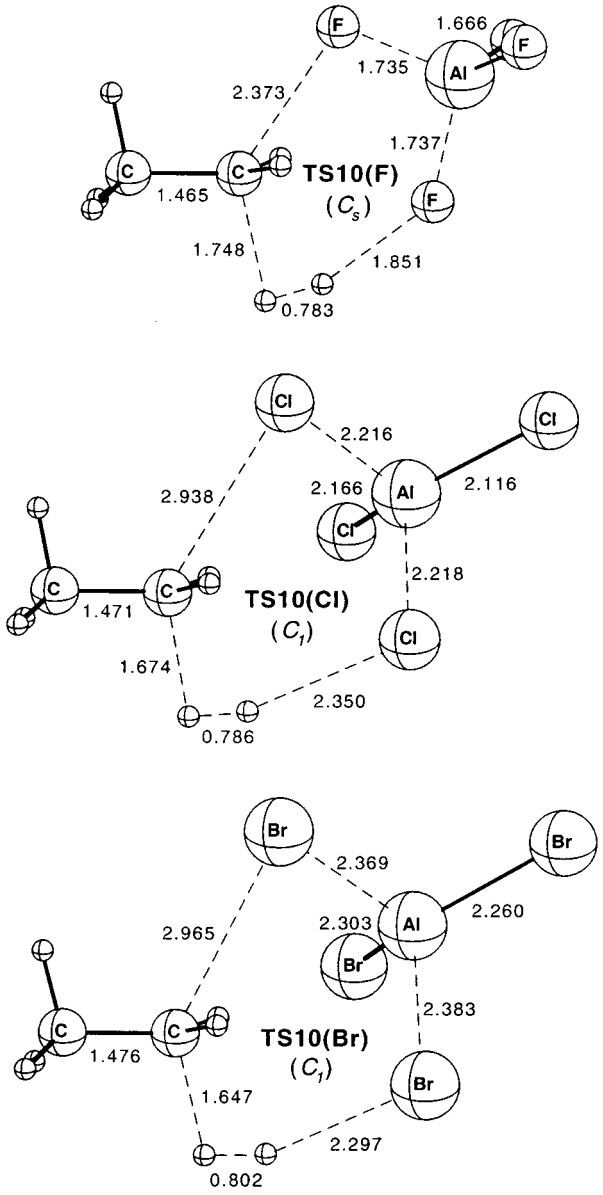

Figure 12. Selected B3-LYP/6-31G(d) bond lengths (Å) for the transition structures **TS10(X)** for the AlX_3-catalyzed hydrogenolyses of the ethyl halides CH_3CH_2X (X = F, Cl, Br).

binding energies for the complexes $[CH_3CH_2X{\cdot}AlX_3]$ at 0 K are 96 kJ mol^{-1} for X = F, 71 kJ mol^{-1} for X = Cl and 65 kJ mol^{-1} for X = Br.

To complete the stepwise hydrogenation of ethene, hydrogenolysis reactions between molecular hydrogen and the complexes $[CH_3CH_2X{\cdot}AlX_3]$ can be formulated. The calculated transition structures **TS10(X)** for these reactions are shown in Figure 12. As in the case of the HX- and AlX_3-catalyzed additions of HX to ethene (Figures 6 and 10), the transition structures for the HX-catalyzed hydrogenolyses of the ethyl halides (**TS8(X)**, Figure 9) and the AlX_3-catalyzed hydrogenolyses of the ethyl halides (**TS10(X)**, Figure 12) have similar geometries. A further similarity is that for the hydrogenolyses of the ethyl halides, as was the case for the additions of HX to ethene, the catalytic effect of AlX_3 is much larger than that of HX. For example, HF catalysis reduces the calculated barrier (compared with the uncatalyzed reaction) for the hydrogenolysis of ethyl fluoride by approximately 12% whereas the presence of AlF_3 leads to a significantly larger reduction of about 50% (cf. Figures 3a, 8a and 11a).

As for the HX- and $(HX)_2$-catalyzed hydrogenations of ethene, there is also a concerted mechanism for the $HAlX_4$-catalyzed reaction that does not involve a CH_3CH_2X-type intermediate. The transition structures **TS11(X)** for the concerted pathway are included in Figure 13. Whereas in the HX-catalyzed concerted hydrogenation (Figure 1) and in the $(HX)_2$-catalyzed hydrogenation via **TS6(X)** (Figure 7), the halogen atoms of the hydrogen halides donate their protons to the double bond and at the same time act as acceptors for the proton resulting from the (formally) heterolytic bond breakage of the H−H bond, these tasks are performed by two different halogen atoms in the $HAlX_4$-catalyzed reaction (Figure 13). In this respect, they bear some similarity to the eight-membered cyclic transition structures **TS7(X)** for the $(HX)_2$-catalyzed reactions shown in Figure 7. Another feature that becomes clear if the transition structures of the concerted $(HX)_2$- and $HAlX_4$-catalyzed hydrogenations of ethene are compared is that the protonation of the double bond is far more advanced in the $HAlX_4$-catalyzed reaction.

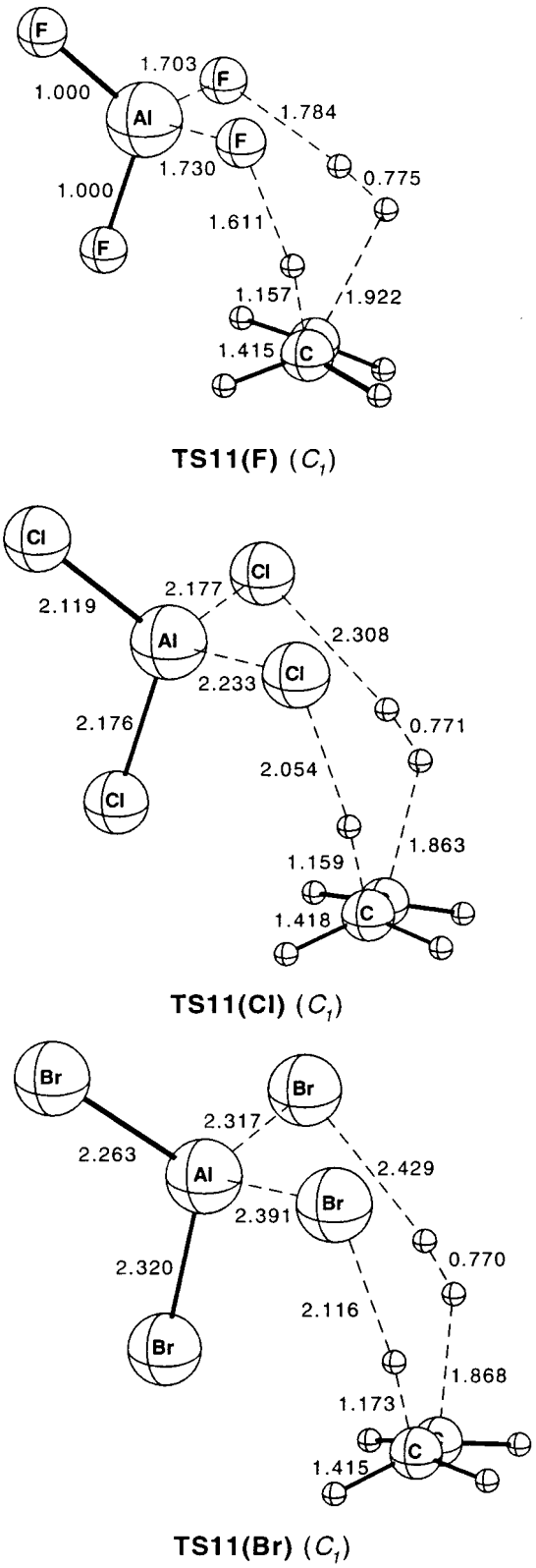

Figure 13. Selected B3-LYP/6-31G(d) bond lengths (Å) for the transition structures **TS11(X)** for the concerted $HAlX_4$-catalyzed hydrogenations of ethene (X = F, Cl, Br).

For example, in the transition structures for the $(HF)_2$-catalyzed hydrogenation, the H−F bond is extended from 0.934 Å in HF (Figure 2) to 1.454 Å in **TS6(F)** and 1.276 Å in **TS7(F)** (Figure 7), and the distances from the proton to the carbon atom are 1.204 and 1.284 Å, respectively. On the other hand, in the transition structure for the $HAlX_4$-catalyzed hydrogenation **TS11(F)**, the H−F bond is lengthened from 0.984 Å in $HAlF_4$ (Figure 2) to 1.611 Å, and the distance from the proton to the carbon atom is much shorter, being only 1.157 Å (Figure 13). In this context, it is also of interest to note that the H−H bond lengths in the molecular hydrogen entities in **TS11(X)** are considerably shorter than in the transition structures **TS6(X)** and **TS7(X)**. As can be seen in Figure 11, the calculated (overall) barriers for the concerted $HAlX_4$-catalyzed hydrogenations of ethene are all less than 100 kJ mol^{-1}, which is a considerable reduction compared with the barrier for the uncatalyzed hydrogenation of 367 kJ mol^{-1} (cf. Table 1).

Whereas the concerted mechanism is clearly energetically favored over the stepwise pathway involving CH_3CH_2X-type intermediates at 0 K for the HX- and $(HX)_2$-catalyzed hydrogenations of ethene (cf. Figures 3 and 8), the situation is different if the reaction is catalyzed by $HAlX_4$. In the latter case, the overall barriers for the concerted and stepwise hydrogenations of ethene are quite close to one another, the maximum difference at 0 K being 23 kJ mol^{-1} in favor of the stepwise mechanism for the $HAlCl_4$-catalyzed hydrogenation (see Figure 11b). The situation at room temperature is basically very similar to that at 0 K, the largest difference of 16 kJ mol^{-1} between the overall free energies of activation for the concerted and stepwise catalytic hydrogenations again being found for the $HAlCl_4$-catalyzed hydrogenation. With such small differences, it is not possible on the basis of our calculations to decide which mechanism will be favored.

Concluding Remarks

In the present investigation, we have applied the MP2/6-311+G(3df,2p)//B3-LYP/6-31G(d) procedure to study the mechanisms of HX-, $(HX)_2$-, and $HAlX_4$-catalyzed hydrogenations of ethene (X = F, Cl, and Br). For all three catalytic reactions, concerted and stepwise mechanisms have been examined. The latter proceed via CH_3CH_2X-type intermediates.

For the HX-catalyzed hydrogenations, our calculations indicate that the concerted mechanism should be energetically favored. Compared with the uncatalyzed hydrogenation of ethene, HX-catalysis reduces the calculated barriers by 28% (HF) to 54% (HBr).

For the $(HX)_2$-catalyzed hydrogenations, there are only slightly larger reductions in the barriers, the theoretical results again favoring the concerted mechanism.

For the $HAlX_4$-catalyzed hydrogenations, the calculated barriers for the concerted and stepwise mechanisms are quite close to one another, so that it is not possible to decide on the basis of our calculations which mechanism will be preferred. The reductions in the barriers through $HAlX_4$-catalysis are much larger than those with HX and $(HX)_2$. For all three $HAlX_4$-catalyzed hydrogenations of ethene, the calculated barriers lie below 100 kJ mol^{-1}, which is a substantial decrease compared with the calculated barrier of 367 kJ mol^{-1} for the uncatalyzed hydrogenation of ethene. In agreement with experimental observations,[6] our calculations indicate that the complexes $HAlCl_4$ and $HAlBr_4$[19] should have potential as transition-metal-free hydrogenation catalysts.

Acknowledgment. We gratefully acknowledge generous allocations of time on the Fujitsu VPP300 and SGI Power Challenge computers of the Australian National University Supercomputing Facility.

Supporting Information Available: GAUSSIAN 98 archive entries for B3-LYP/6-31G(d) optimized geometries of relevant

equilibrium structures and transition structures (Table S1), and calculated B3-LYP/6-31G(d) total energies and ZPVEs and MP2/6-311+G(3df,2p)//B3-LYP/6-31G(d) total energies (Table S2) (a total of 17 pages). This material is available free of charge via the Internet at http://pubs.acs.org.

References and Notes

(1) Chaloner, P. A.; Esteruelas, M. A.; Ferenc, J.; Oro, L. A. *Homogeneous Hydrogenation*; Kluwer Academic Publishers: Dordrecht, 1994.

(2) (a) Rylander, P. N. *Catalytic Hydrogenation over Platinum Metals*; Academic Press: New York, 1967. (b) Bond, G. C. *Catalysis by Metals*; Academic Press: London, 1962. (c) Zaera, F. *Langmuir* **1996**, *12*, 88−94.

(3) (a) Farrauto, R. J.; Batholomew, C. H. *Fundamentals of Industrial Catalytic Processes*; Blackie Academic & Professional: London, 1997. (b) Roessler, F. *Chimia* **1996**, *50*, 106−109. (c) Schmid, R. *Chimia* **1996**, *50*, 110−113.

(4) Bader, R. R.; Baumeister, P.; Blaser, H.-U. *Chimia* **1996**, *50*, 99−105.

(5) Walling, C.; Bollyky, L. *J. Am. Chem. Soc.* **1961**, *83*, 2968−2969.

(6) Walling, C.; Bollyky, L. *J. Am. Chem. Soc.* **1964**, *86*, 3750−3752.

(7) Siria, J. C.; Duran, M.; Lledós, A.; Bertrán, J. *J. Am. Chem. Soc.* **1987**, *109*, 7623−7629.

(8) Scott, A. P.; Golding, B. T.; Radom, L. *New J. Chem.* **1998**, 1171−1173.

(9) Senger, S.; Radom, L. *J. Am. Chem. Soc.* In press.

(10) Hehre, W. J.; Radom, L.; Schleyer, P. v. R.; Pople, J. A. *Ab Initio Molecular Orbital Theory*; Wiley: New York, 1986.

(11) Jensen, F. *Introduction to Computational Chemistry*; Wiley: Chichester, 1998.

(12) Frisch, G. W.; Trucks, G. W.; Schlegel, H. B.; Scuseria, G. E.; Robb, M. A.; Cheeseman, J. R.; Zakrzewski, V. G.; Montgomery, Jr., J. A.; Stratmann, R. E.; Burant, J. C.; Dapprich, S.; Millam, J. M.; Daniels, A. D.; Kudin, K. N.; Strain, M. C.; Farkas, O.; Tomasi, J.; Barone, V.; Cossi, M.; Cammi, R.; Mennucci, B.; Pomelli, C.; Adamo, C.; Clifford, S.; Ochterski, J.; Petersson, G. A.; Ayala, P. Y.; Cui, Q.; Morokuma, K.; Malick, D. K.; Rabuck, A. D.; Raghavachari, K.; Foresman, J. B.; Cioslowski, J.; Ortiz, J. V.; Stefanov, B. B.; Liu, G.; Liashenko, A.; Piskorz, P.; Komaromi, I.; Gomperts, R.; Martin, R. L.; Fox, D. J.; Keith, T.; Al-Laham, M. A.; Peng, C. Y.; Nanayakkara, A.; Gonzalez, C.; Challacombe, M.; Gill, P. M. W.; Johnson, B.; Chen, W.; Wong, M. W.; Andres, J. L.; Gonzalez, C.; Head-Gordon, M.; Replogle, E. S.; Pople, J. A. *GAUSSIAN 98*, Revision A.6; Gaussian Inc., Pittsburgh, PA, 1998.

(13) Scott, A. P.; Radom, L. *J. Phys. Chem.* **1996**, *100*, 16502−16513.

(14) (a) Clavero, C.; Duran, M.; Lledós, A.; Ventura, O. N.: Bertrán, J. *J. Am. Chem. Soc.* **1986**, *108*, 923−928. (b) Clavero, C.; Duran, M.; Lledós, A.; Ventura, O. N.: Bertrán, J. *J. Comput. Chem.* **1987**, *8*, 481−488.

(15) Menéndez, M. I.; Suárez, D.; Sordo, J. A.; Sordo, T. L. *J. Comput. Chem.* **1995**, *16*, 659−666.

(16) The MP2/6-311+G(3df,2p)//B3-LYP/6-31G(d) single-point energy of the chlorine analogue of the C_s symmetrical **TS4(Br)** (with two imaginary frequencies at the B3-LYP/6-31G(d) level) is 11 kJ mol^{-1} higher than the corresponding energy for the C_1 transition structure **TS4(Cl)** (cf. Figure 5).

(17) Curtiss, L. A.; Scholz, G. *Chem. Phys. Lett.* **1993**, *205*, 550−554.

(18) Scholz, G. *J. Mol. Struct. (THEOCHEM)* **1994**, *309*, 227−234.

(19) Practical considerations are not in favor of $HAlF_4$ as a transition-metal-free hydrogenation catalyst because AlF_3 is insoluble even in concentrated HF.